WATER TREATMENT

Chloronitramide anion is a decomposition product of inorganic chloramines

Julian L. Fairey[1]*†‡, Juliana R. Laszakovits[2]‡, Huong T. Pham[1]§, Thien D. Do[1]¶, Samuel D. Hodges[1]#, Kristopher McNeill[2]*, David G. Wahman[3]*

Inorganic chloramines are commonly used drinking water disinfectants intended to safeguard public health and curb regulated disinfection by-product formation. However, inorganic chloramines themselves produce by-products that are poorly characterized. We report chloronitramide anion ($Cl–N–NO_2^-$) as a previously unidentified end product of inorganic chloramine decomposition. Analysis of chloraminated US drinking waters found $Cl–N–NO_2^-$ in all samples tested (n = 40), with a median concentration of 23 micrograms per liter and first and third quartiles of 1.3 and 92 micrograms per liter, respectively. $Cl–N–NO_2^-$ warrants occurrence and toxicity studies in chloraminated water systems that serve more than 113 million people in the US alone.

For >100 years, drinking water disinfection, primarily with chlorine, has been used to inactivate pathogens to curb waterborne disease and safeguard public health (*1*). However despite its efficacy as a disinfectant, chlorine reacts with natural and anthropogenic organic matter, bromide, and iodide to form disinfection by-products (*2*, *3*) that have been associated with bladder and colon cancer (*4*, *5*), low birth weight (*6*), and miscarriage (*7*). Of the estimated 600 to 700 disinfection by-products identified over the past 50 years (*3*), trihalomethanes and haloacetic acids are the predominant compounds formed on a mass basis during chlorine disinfection, and they are regulated in the US by the Environmental Protection Agency (EPA) (*8*). Since promulgation of the 1998 EPA Stage 1 Disinfectants and Disinfection Byproducts Rule (*9*), many public water systems have switched to alternative disinfectants, including inorganic chloramines (*10*). Recent surveys of US drinking water systems estimate that >113 million people are supplied chloraminated drinking water (*11*). Although inorganic chloramines form fewer regulated disinfection by-products, they may enhance the formation of other disinfection by-products, including those containing nitrogen, which may be more toxicologically relevant (*12*).

[1]Department of Civil Engineering, University of Arkansas, Fayetteville, AR 72701, USA. [2]Institute of Biogeochemistry and Pollutant Dynamics, ETH Zurich, 8092 Zurich, Switzerland. [3]Center for Environmental Solutions & Emergency Response, Office of Research and Development, US Environmental Protection Agency, Cincinnati, OH 45268, USA.
*Corresponding author. Email: julianf@uark.edu (J.L.F.); kristopher.mcneill@env.ethz.ch (K.M.); wahman.david@epa.gov (D.G.W.)
†Visiting professor during conceptualization and investigation at ETH Zurich and Eawag, Swiss Federal Institute of Aquatic Science and Technology, Duebendorf 8600, Switzerland.
‡These authors contributed equally to this work.
§Present address: Nine South Estate, Phuoc Kien, Nha Be District, Ho Chi Minh City, Vietnam.
¶Present address: Ho Chi Minh City University of Natural Resources and Environment, Tan Binh District, Ho Chi Minh City, Vietnam.
#Present address: Department of Civil and Environmental Engineering, Christian Brothers University, Memphis, TN, 38104 USA.

When using inorganic chloramines in drinking water, monochloramine (NH_2Cl) is the predominant species and reacts with drinking water constituents (e.g., natural organic matter, NOM) or decomposes through dichloramine ($NHCl_2$) to end products that include nitrogen gas, nitrite (NO_2^-), and nitrate (NO_3^-) (*13*, *14*). An inorganic chloramine kinetic model (*15*, *16*) has long been used to simulate NH_2Cl and $NHCl_2$ concentrations, but further kinetic model refinements are required to delineate disinfection by-product formation pathways and to develop generalizable control strategies. Specifically, accounting for inorganic chloramine decomposition intermediates and minor end-products remains incomplete (*17*). One unknown inorganic chloramine decomposition end product was first detected >40 years ago as an ultraviolet (UV) absorbance interference while kinetically monitoring NH_2Cl and $NHCl_2$ (*18*). This so-called unidentified product (UP) was subsequently observed from $NHCl_2$ decomposition using liquid chromatography (*19*), and was then shown to also form during NH_2Cl decomposition (*19*, *20*).

Previous efforts to characterize the UP have used two inorganic chloramine decomposition methods for UP formation (*20*), which are fast (over hours) pH cycling starting with $NHCl_2$ or slow (over days to weeks) NH_2Cl decomposition. In the former method, the pH of an initially pure NH_2Cl solution is lowered to pH 3 to 4, creating a pure $NHCl_2$ solution. Then, the $NHCl_2$ solution is subjected to repeated pH cycling between high and low pH. At high pH (i.e., pH 9 to 10), some $NHCl_2$ converts to NH_2Cl, whereas most $NHCl_2$ decomposes through base-catalyzed hydrolysis, resulting in UP formation. At low pH (i.e., pH 3 to 4), any remaining NH_2Cl converts back to $NHCl_2$. For the slow NH_2Cl decomposition method, a pure NH_2Cl solution is adjusted to a drinking water–relevant pH (i.e., pH 7 to 9). Then, the NH_2Cl slowly converts to $NHCl_2$ which decomposes through based-catalyzed hydrolysis, resulting in UP formation. Using the formed UP, subsequent photolysis and [illegible] fite destruction experiments found that the [illegible] likely contains one or two atoms of chlorine and nitrogen (*20*). Concerningly, the inorganic chloramine decomposition and UP destruction experiments demonstrated that UP formation was 4 to 5% of the total inorganic chloramine concentration decomposed (*21*). This finding suggests that the UP may form at microgram per liter levels in chloraminated drinking waters, like regulated trihalomethanes and haloacetic acids (*22*). Subsequent UP characterization efforts showed that the UP did not partition into organic solvents and was strongly retained by anion exchange resins but could not be eluted, indicating that it had a large selectivity coefficient and/or may have reacted with the tertiary and quaternary ammonium exchange groups on the resins (*23*). Prior toxicity studies are therefore unlikely to have included the UP because of their reliance on resins and organic solvents to formulate enriched disinfection by-product mixtures for bioassays [e.g., (*24*)].

Despite being able to reproducibly form the UP for >30 years, prior characterization efforts (*20*, *21*, *23*, *25*) were stymied by analytical limitations and an incomplete understanding of inorganic chloramine decomposition chemistry and UP formation, which we have worked to address (*14*, *17*). Specifically, we reported that the product of $NHCl_2$ hydrolysis was nitroxyl (HNO) which reacts with dissolved oxygen to form peroxynitrite (ONOOH) (*14*). Adding HNO and ONOOH chemistries to the inorganic chloramine kinetic model (*15*, *16*) demonstrated their roles as key intermediates in the formation of *N*-nitrosodimethylamine (*14*), an unregulated disinfection by-product of human health concern associated with inorganic chloramine use (*26*). We later showed that UP formation was dependent on dissolved oxygen (*17*) and was likely formed by inorganic chloramine species reacting with ONOOH decomposition products (e.g., $NO_2^{\bullet}$, N_2O_4, or NO_2^+) which would otherwise form NO_3^- (*27*). Identifying the UP could (i) spur occurrence and toxicity studies to assess its public health risk in drinking water and (ii) facilitate completion of the inorganic chloramine kinetic model (*14*), which is needed to assess the formation and control of disinfection by-products to improve drinking water quality in systems using inorganic chloramines.

UP formation

Following previous work (*20*, *23*), the UP was formed by two known methods: slow NH_2Cl decomposition and fast pH cycling starting with $NHCl_2$ (see the supplementary materials). For the first method, the UP was formed in the absence and presence of a reconstituted (*28*) riverine NOM. The UP was absent on the ion chromatography (IC) conductivity chromatogram, presumably due to its low concentration (fig. S1A), but it was present on IC absorbance

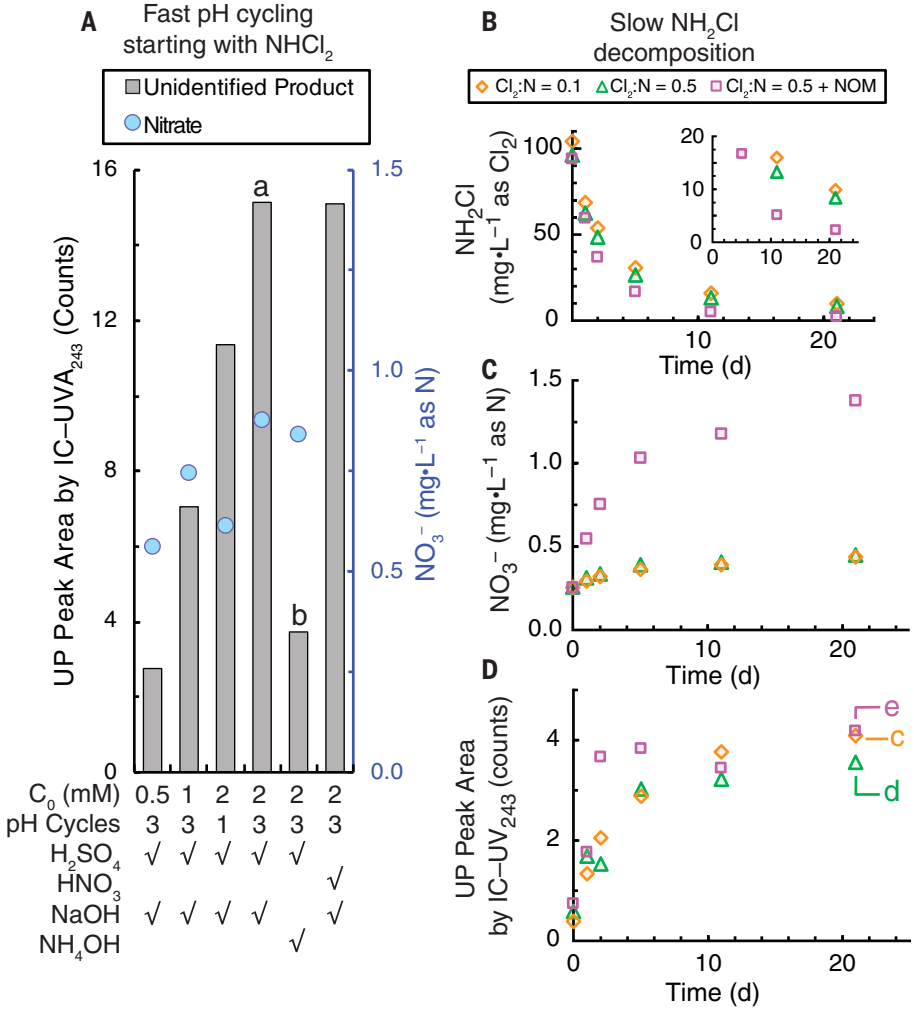

Fig. 1. UP formation from inorganic chloramine decomposition. (**A**) UP and NO_3^- formation from fast pH cycling starting with initial $NHCl_2$ concentrations (C_0) of 0.5, 1, or 2 mM and one or three pH cycles between pH 3.7 to 4.0 and 9.5. H_2SO_4 or HNO_3 was used to decrease pH and NaOH or NH_4OH was used to increase pH, as indicated by the check mark below each bar. For the sample formulated with HNO_3, NO_3^- was 440 mg/liter N and is not shown due to scaling. (**B**) Slow decomposition of 1.5 mM NH_2Cl over 21 days at pH 7.5 and an initial Cl_2:N [mol Cl_2•(mol N)$^{-1}$] of 0.1, 0.5, and 0.5 + NOM, in which the NOM concentration was 50 mg/liter as C dissolved organic carbon and the inset magnifies the NH_2Cl data <20 mg/liter Cl_2. (**C** and **D**) Corresponding formation of NO_3^- (C) and UP (D). Lowercase letters in (A) and (D) indicate the samples used to determine the UP unequivocal ionic formula (Fig. 2 and figs. S3 to S7).

chromatograms at 243 nm (IC-UV_{243}; see the supplementary materials and fig. S1B), eluting at ~49 min.

UP formation from fast pH cycling starting with $NHCl_2$ was proportional to the initial $NHCl_2$ concentration and increased with the number of pH cycles. UP peak area by IC-UV_{243} increased fivefold as the initial $NHCl_2$ concentration increased from 0.5 to 2 mM (Fig. 1A). For the initial 2 mM $NHCl_2$ concentration, the UP formation was ~11 counts after one pH cycle and 15 counts after three pH cycles, consistent with prior work (*23*) showing incomplete $NHCl_2$ decomposition after one pH cycle. Decreasing the pH with HNO_3 resulted in similar UP formation compared with H_2SO_4 and indicated excess NO_3^- (e.g., 440 mg/liter as N) did not affect UP formation. Increasing the pH with NH_4OH instead of NaOH, however, decreased the UP formation about threefold.

UP formation from slow decomposition of 1.5 mM NH_2Cl at pH 7.5 was monitored over 21 days for an initial chlorine to ammonia-nitrogen molar ratio (Cl_2:N) of 0.1 and 0.5 mol Cl_2•(mol N)$^{-1}$, like prior work (*20*). The Cl_2:N ratio represents the amount of free chlorine and free ammonia used to form inorganic chloramines. To assess the plausibility of drinking water UP formation where NOM is typically present, an initial Cl_2:N of 0.5 mol Cl_2•(mol N)$^{-1}$ was monitored with NOM added at 50 mg/liter dissolved organic carbon (DOC) as carbon. Although this DOC level is about an order of magnitude greater than that of most drinking waters, the initial NH_2Cl to DOC mass ratio (Cl_2:DOC) was ~2, which is typical of US drinking water systems (*29*). Without NOM, and as expected based on known inorganic chloramine chemistry (*16*), NH_2Cl decomposition was similar for an initial Cl_2:N of 0.1 and 0.5 mol Cl_2•(mol N)$^{-1}$ (Fig. 1B). For an initial Cl_2:N of 0.5 mol Cl_2•(mol N)$^{-1}$ with added NOM (0.5 + NOM), NH_2Cl decomposition was greater and faster (Fig. 1B, inset), indicating that NOM accelerated NH_2Cl decomposition, like in natural waters [e.g., (*30*)]. NO_3^- increased from ~0.3 to 0.5 mg/liter as N over 21 days for an initial Cl_2:N of 0.1 and 0.5 mol Cl_2•(mol N)$^{-1}$ (Fig. 1C) and from ~0.3 to 1.4 mg/liter as N for the 0.5 + NOM condition. These results were consistent with previous work showing that NOM reacts with NH_2Cl to form more NO_3^- and free ammonia but less nitrogen gas (*31*). UP formation increased over 21 days to ~4 counts and was similar at an initial Cl_2:N of 0.1 and 0.5 mol Cl_2•(mol N)$^{-1}$ (Fig. 1D), like previous results (*20*), indicating that excess free ammonia did not affect UP formation during slow NH_2Cl decomposition. Figure S2 shows a direct linear relationship between UP peak area and NH_2Cl decomposed for the initial Cl_2:N of 0.1 and 0.5 mol Cl_2•(mol N)$^{-1}$ with an R^2 of 0.96 (n = 12). The UP peak area for the Cl_2:N = 0.5 + NOM treatment was greater than or within the best-fit line 95% confidence interval, suggesting the reactive nitrogen species involved in UP formation (*17*) were not quenched by NOM at an initial Cl_2:DOC ratio relevant to drinking water (*32*).

UP unequivocal ionic formula

IC–negative mode electrospray ionization–ultra-high-resolution mass spectrometry (IC–ESI–UHRMS; see the supplementary materials) was used to separate the UP from chloride, sulfate, and phosphate anions to determine its accurate mass-to-charge ratio (m/z) and isotopic distribution. The UP eluted between sulfate and phosphate at an elution time of 10.2 min (Fig. 2A). For sample a in Fig. 1A, the most abundant ion measured at an elution time of 10.2 min (Fig. 2B) had an m/z of 94.9655 (Fig. 2C), which closely matches the theoretical m/z for monoisotopic $ClN_2O_2^-$ (*33*) (see the supplementary materials). Excellent agreements were observed between the measured and theoretical m/z values for ^{37}Cl (Fig. 2C), ^{18}O (Fig. 2C), ^{15}N (Fig. 2D), and ^{17}O (Fig. 2D) isotopes, with mass deviations (Δm) of 1.053 ppm or less. Furthermore, their respective relative abundances were in excellent agreement (Fig. 2E), particularly given the low abundances (<1%) of the ^{15}N, ^{18}O, and ^{17}O isotopes. Similar plots are shown for the other four UP samples marked with lowercase letters in Fig. 1, A and D, which

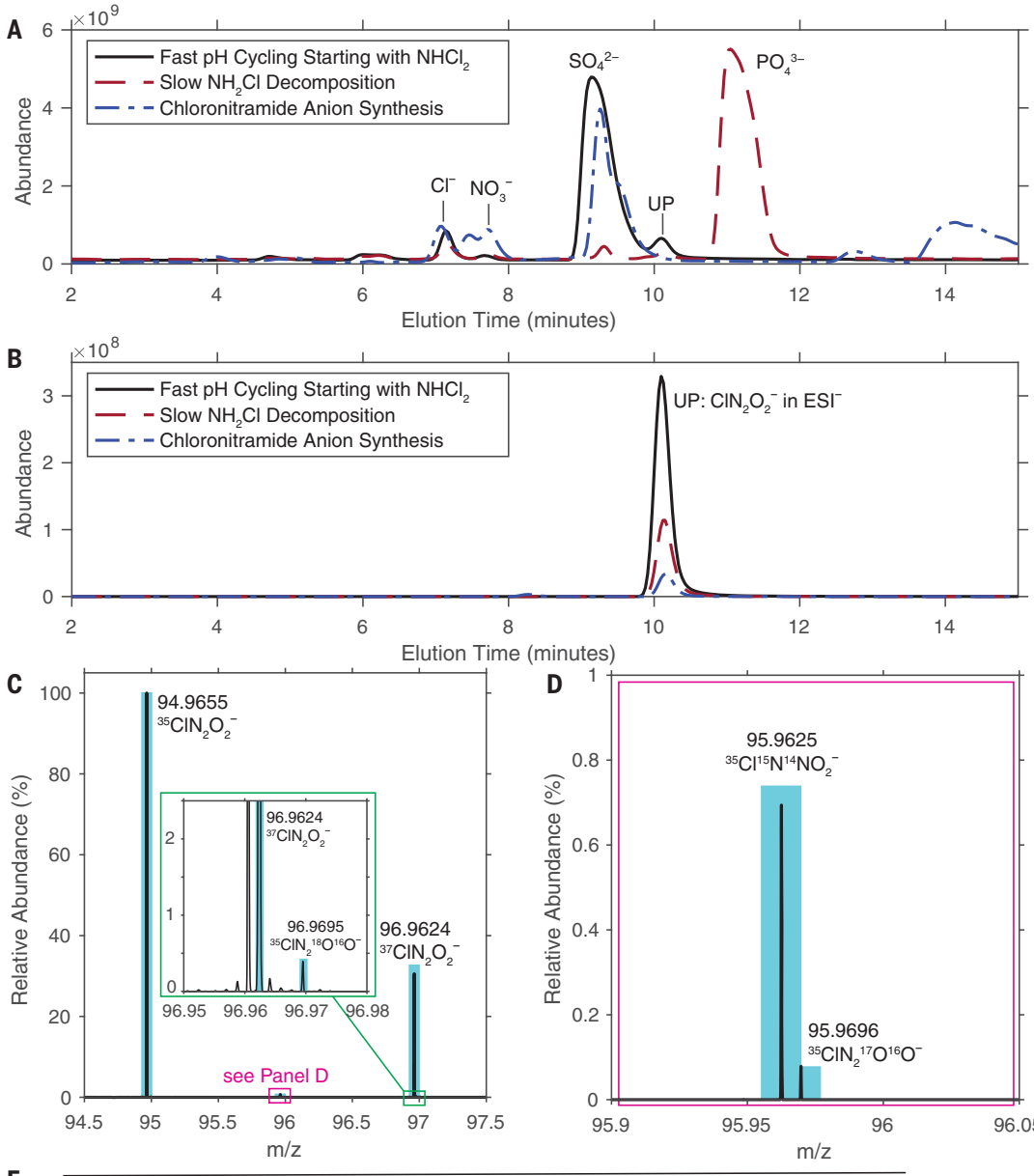

Fig. 2. UP accurate mass and ion peaks in MS spectra indicating that the unequivocal molecular formula is $ClN_2O_2^-$. (**A**) Total ion count from IC-ESI-UHRMS chromatograms. Solid black line indicates fast pH cycling starting with $NHCl_2$ (Fig. 1A, sample a); dashed maroon line indicates slow NH_2Cl decomposition (Fig. 1D, sample e); and dash-dot blue line indicates Cl–N–NO_2^- synthesis. (**B**) UP selected ion chromatograms of peak at *m/z* = 94.9654 from fast pH cycling starting with $NHCl_2$ (Fig. 1A, sample a), slow NH_2Cl decomposition (Fig. 1D, sample e), and Cl–N–NO_2^- synthesis had matching elution times of 10.2 min. (**C** and **D**) Theoretical isotopic pattern (*33*) (cyan bars) and measured ions (black spikes) from fast pH cycling starting with $NHCl_2$ (Fig. 1A, sample a) of $^{35}ClN_2O_2^-$ (Δm = 1.053 ppm), $^{37}ClN_2O_2^-$ (Δm = 0.000 ppm), and $^{35}ClN_2{}^{18}O^{16}O^-$ (Δm = 1.031 ppm) (C) and $^{35}Cl^{15}N^{14}NO_2^-$ (Δm = 1.042 ppm) and $^{35}ClN_2{}^{17}O^{16}O^-$ (Δm = 0.000 ppm) (D). (**E**) Measured and theoretical *m/z* and relative abundances of ion peaks in MS spectra from fast pH cycling starting with $NHCl_2$ (Fig. 1A, sample a).

E

Ion	m/z		Relative Abundance (%)	
	Measured	Theoretical	Measured	Theoretical
$^{35}ClN_2O_2^-$	94.9655	94.9654	100	100
$^{37}ClN_2O_2^-$	96.9624	96.9624	31	33
$^{35}Cl^{15}N^{14}NO_2^-$	95.9625	95.9624	0.69	0.74
$^{35}ClN_2{}^{18}O^{16}O^-$	96.9695	96.9696	0.40	0.42
$^{35}ClN_2{}^{17}O^{16}O^-$	95.9696	95.9696	0.072	0.077

included the 2 mM $NHCl_2$ sample formulated with H_2SO_4 and NH_4OH (fig. S3) and the three samples formulated by slow NH_2Cl decomposition at an initial Cl_2:N of 0.1 mol Cl_2•(mol N)$^{-1}$ (fig. S4), 0.5 mol Cl_2•(mol N)$^{-1}$ (fig. S5), and 0.5 mol Cl_2•(mol N)$^{-1}$ with added NOM (fig. S6). These results demonstrate that the same UP formed from fast pH cycling starting with $NHCl_2$ and slow NH_2Cl decomposition. $ClN_2O_2^-$ fragmentation was attempted at a normalized collision energy of 120%, but was not successful, a logical result given the low UP *m/z* (<100) relative to the 50 *m/z* fragment cutoff. The UP was also observed by direct infusion ESI–UHRMS (fig. S7), bypassing the IC separation, which confirmed that it was not formed as a reaction product on the anion exchange resin as was previously speculated (*23*). This evidence supports the assertion that the unequivocal UP ionic formula is $ClN_2O_2^-$.

Cl–N–NO_2^- synthesis and formation pathway

The UP was synthesized (Fig. 3A, pathway f, and see the supplementary materials and figs. S8 and S9) based on a plausible formation pathway with the nitronium cation (NO_2^+) as the key intermediate (*17*). A hypothesized structure of Cl–N–NO_2^-

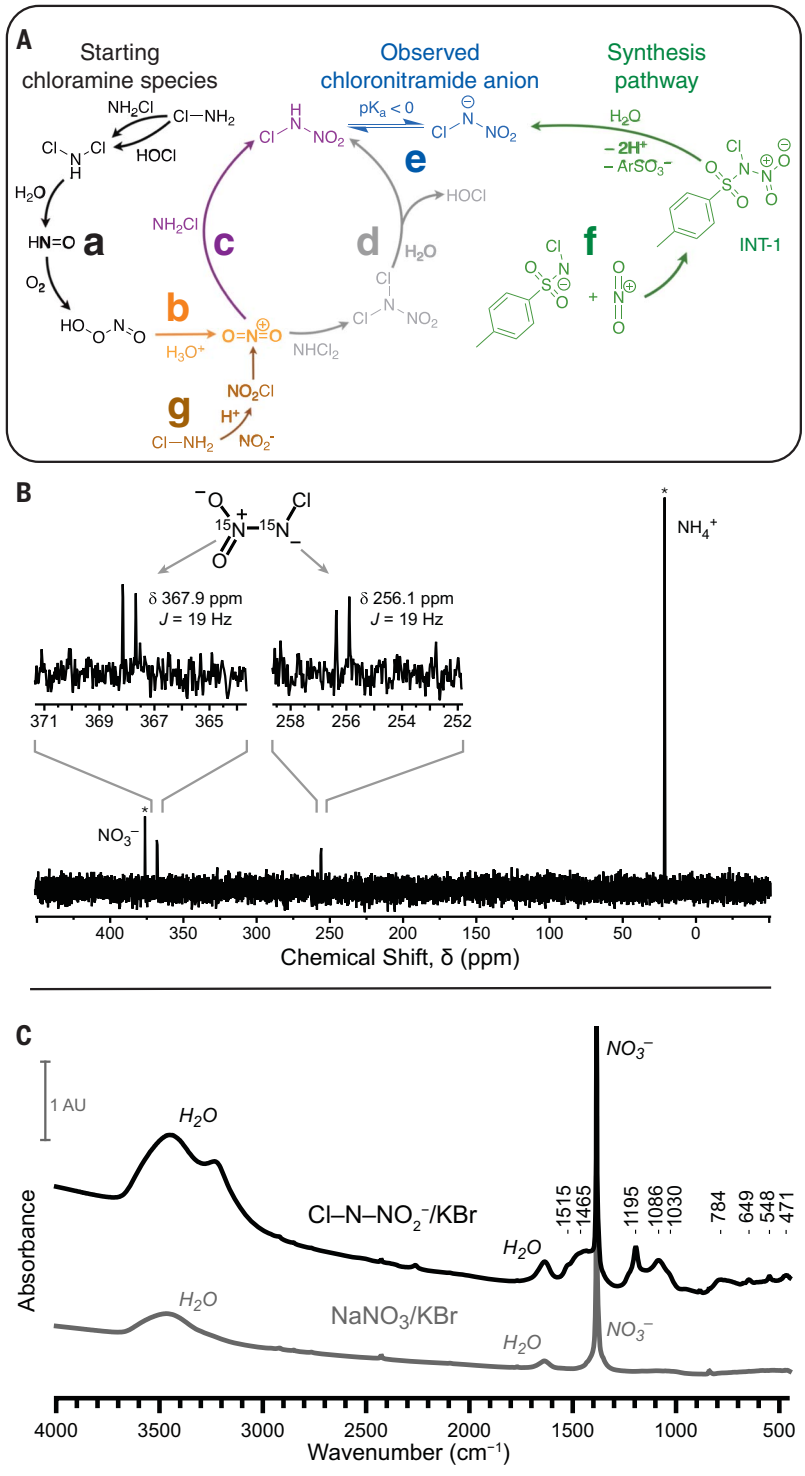

Fig. 3. Proposed Cl–N–NO_2^- formation and synthesis pathways, ^{15}N NMR spectrum of dual-labeled Cl–N–NO_2^-, and FTIR spectrum of unlabeled Cl–N–NO_2^-. (**A**) Pathway a (black) shows NH_2Cl decomposition to $NHCl_2$ in the presence of excess ammonia (*35*) followed by $NHCl_2$ hydrolysis to HNO (*14*) and reaction with O_2 to ONOOH (*36*). Pathway b (orange) shows ONOOH decomposition (*27*) to NO_2^+, the proposed key intermediate and nitrating agent. NO_2^+ reacts with NH_2Cl and $NHCl_2$ in pathways c (purple) and d (gray), respectively, to form Cl–HN–NO_2^-, which dissociates to Cl–N–NO_2^- in pathway e (blue). Pathway f (green) shows Cl–N–NO_2^- synthesis (see figs. S8 and S9 for details) from chloramine-T (*62*) and NO_2^+ to an intermediate *N*-chloro-*N*-nitro-*p*-toluenesulfonamide (INT-1) that undergoes hydrolysis (H_2O), deprotonation (– $2H^+$), and tosic acid loss (– $ArSO_3^-$) to Cl–N–NO_2^- in pathway e (blue). Pathway g (brown) shows NH_2Cl reaction with H^+ and NO_2^- to NO_2Cl, followed by decomposition to NO_2^+, feeding into pathway c and/or d. (**B**) ^{15}N NMR spectrum of dual-^{15}N-labeled Cl–N–NO_2^- whole-water sample produced using Cl–N–NO_2^- formation method 3C (see the supplementary materials) containing species including NH_4^+/NH_3, NO_3^-, NO_2^-, and chloride. With the spectrum referenced to liquid ammonia (δ = 0 ppm) using the NO_3^- peak in the sample (δ = 376.5 ppm) (*38*), the resonances at δ = 367.9 ppm and 256.1 ppm are assigned to the nitro and the amide nitrogen atoms, respectively. (**C**) FTIR spectrum of unlabeled Cl–N–NO_2^- measured in a KBr pellet after lyophilization of a Cl–N–NO_2^- isolate produced by formation method 3A (see the supplementary materials) showing bands consistent with NO_2 stretching modes (1465 and 1195 cm^{-1}) and the N–N stretching mode (1086 cm^{-1}), with NO_3^- present as a background contaminant. $NaNO_3$ spectrum is shown to control for NO_3^-. AU, absorbance unit; chloramine-T, sodium *N*-chloro-*p*-toluenesulfonamide.

was initially proposed based on the experimental context in which the UP was formed using multiple lines of evidence (*34*). Under drinking water conditions in which excess ammonia is present, pathway a (Fig. 3A) is the intrinsic NH_2Cl decomposition pathway, occurring in parallel with NH_2Cl demand reactions from water constituents such as NOM (*35*). In pathway a, NH_2Cl decomposes to $NHCl_2$, followed by $NHCl_2$ hydrolysis to HNO (*14*). Some HNO reacts with dissolved oxygen to form ONOOH (*36*), which is unstable and decomposes through various reactive nitrogen species to NO_2^- and NO_3^- (*27*). NO_2^+ (Fig. 3A, pathway b) was hypothesized as the nitrating agent, formed by ONOOH decomposition (*37*). We posit a NO_2^+ reaction with NH_2Cl (Fig. 3A, pathway c) or $NHCl_2$ followed by hydrolysis (Fig. 3A, pathway d), forming chloronitramide (Cl–NH–NO_2), which dissociates to Cl–N–NO_2^- (Fig. 3A, pathway e).

Cl–N–NO_2^- structural confirmation, molar absorptivity, and photolysis pathway

To generate sufficient Cl–N–NO_2^- for spectroscopic characterization, three Cl–N–NO_2^- formation methods (including mono– and dual–^{15}N-labeled Cl–N–NO_2^- versions) were developed

(see the supplementary materials) with subsequent Cl–N–NO_2^- isolation by IC (see the supplementary materials) and confirmation by hydrophilic interaction liquid chromatography UHRMS (see the supplementary materials and figs. S10 to S16). Cl–N–NO_2^- concentrations were greatest for Cl–N–NO_2^- formation method 3 [Fig. 3A, pathway g (intended) and Fig. 3A pathways a and b (adventitious) and fig. S17A], which was therefore used for structural confirmation by ^{15}N nuclear magnetic resonance (^{15}N NMR; see the supplementary materials) and Fourier transform infrared (FTIR; see the supplementary materials) spectroscopy and to determine the Cl–N–NO_2^- molar absorptivity (ε) for reference material standardization (see the supplementary materials). The ^{15}N NMR spectrum of Cl–N–NO_2^- (Fig. 3B) shows two doublets with a ^{15}N–^{15}N one-bond coupling constant of ^1J = 19 Hz. With the spectrum referenced to liquid ammonia (δ = 0 ppm) using the NO_3^- peak in the sample (δ = 376.5 ppm) (*38*), the downfield resonance of δ = 367.9 ppm is assigned to the nitro N atom and the upfield resonance at δ = 256.1 ppm to the amide N atom. The spectrum has notable similarities to that reported for the dinitramide ion, $N(NO_2)_2^-$, specifically the nitro ^{15}N resonance at δ = 367.5 ppm and the ^{15}N–^{15}N ^1J = 19.3 Hz (*39*). The amide ^{15}N resonance of $N(NO_2)_2^-$ (δ = 321.4 ppm) is downfield of the amide resonance of Cl–N–NO_2^-, reflecting the stronger electron-withdrawing effect of the nitro compared with the chloro substituent. The FTIR spectrum of Cl–N–NO_2^- (Fig. 3C) shows strong absorption bands at 1465, 1195, and 1080 cm^{-1}. Compared with previous studies on $N(NO_2)_2^-$ (*39*, *40*), these bands are tentatively assigned to the NO_2 asymmetric stretch, the NO_2 symmetric stretch, and the N–N stretch, respectively. The Cl–N–NO_2^- isolate ε spectrum was determined between 190 to 290 nm by photolysis at 254 nm (Fig. 4A and supplementary materials), resulting in an ε at 243 ($ε_{243}$) of 5310 ± 170 $M^{-1}•cm^{-1}$ (95% confidence interval), which is within 6% of the $ε_{243}$ of 5000 $M^{-1}•cm^{-1}$ estimated for the UP by others (*20*). Subsequently, we posited a proposed photolysis pathway that included chloride, NO_2^-, and nitrous oxide (N_2O) as end products (Fig. 4B and supplementary materials) that was validated with additional photolysis experiments at 254 nm (see the supplementary materials), where the expected 2:1 molar ratio was observed for formed NO_2^- to formed N_2O (average 1.9 ± 0.2 molar ratio; Fig. 4C, supplementary materials, and table S1). The formation of chloride, NO_2^-, and N_2O as Cl–N–NO_2^- photolysis products (Fig. 4 and figs. S18 and S19) provides additional evidence for the Cl–N–NO_2^- structural assignment. There are two important resonance structures for this anion (fig. S20), one with an N=O double bond [chloro(nitro)azanide] and one with an N=N double bond [chloroimino(dioxido)azanium]. Future work is needed to determine which structure is a better description of the compound.

Environmental relevance of Cl–N–NO_2^- in chloraminated drinking waters

Given Cl–N–NO_2^- presence in archived samples (see the supplementary materials and table S2), additional sampling was completed in chloraminated drinking water systems (see the supplementary materials and table S3). Cl–N–NO_2^- was not quantifiable (0.17 μg/liter limit of detection and 0.58 μg/liter limit of quantitation) in negative controls in three systems from cantons in Switzerland that did not use chlorine-based disinfectants. By contrast, Cl–N–NO_2^- was detected in all samples (n = 40) from 10 chloraminated US drinking water systems (23 μg/liter median, 120 μg/liter maximum, and 1.3 and 92 μg/liter first and third quartiles, respectively). The coefficient of variation among the samples from a given residence (n = 4) was 2 to 24% with a median of 5%. The results indicated that Cl–N–NO_2^- may persist in

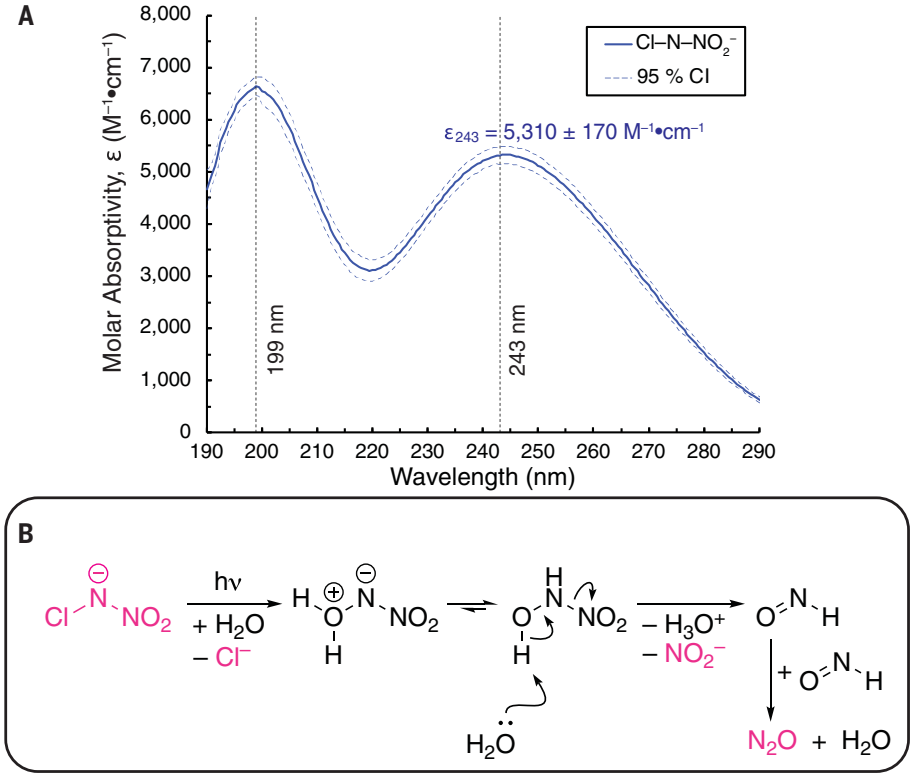

C

Initial Cl–N–NO_2^- Level	Replicate	NO_2^- Formed to N_2O Formed (mol/mol)	NO_2^- Formed to Cl–N–NO_2^- Destroyed (mol/mol)
Low	1	1.9	1.3
	2	1.9	1.2
Medium	1	1.8	1.1
	2	1.5	1.0
High	1	2.1	1.1
	2	1.9	1.1
Average ± 95 % CI =		**1.9 ± 0.2**	**1.1 ± 0.1**

Fig. 4. Cl–N–NO_2^- molar absorptivity spectra, proposed Cl–N–NO_2^- pathway from photolysis at 254 nm and summary of Cl–N–NO_2^- photolysis experiments at 254 nm focused on N_2O formation. (**A**) Determined Cl–N–NO_2^- molar absorptivity (ε) and associated 95% confidence interval from Cl–N–NO_2^- photolysis at 254 nm experiments where chloride release was correlated with absorbance loss at 243 nm. (**B**) Proposed Cl–N–NO_2^- photolysis at 254 nm pathway where experimentally quantified reactants and products are denoted in pink. Photolysis at 254 nm leads to initial, successive release of Cl^-, NO_2^-, and HNO, with HNO subsequently reacting with a second HNO to form N_2O. (**C**) Summary of the molar ratios of NO_2^- formed to N_2O formed and NO_2^- formed to Cl–N–NO_2^- destroyed from duplicate N_2O-focused Cl–N–NO_2^- photolysis at 254 nm experiments conducted at three initial Cl–N–NO_2^- levels (table S1).

chloraminated drinking waters, and Cl–N–NO_2^- concentrations may be greater than many currently regulated disinfection by-products on a molar basis (average molecular weight = 95.45 g•mol^{-1}) and on a mass basis. Given that the Cl–N–NO_2^- concentration is proportional to inorganic chloramine decomposition (Fig. 1 and fig. S2), Cl–N–NO_2^- concentrations would presumably increase with ongoing efforts to emphasize greater inorganic chloramine concentrations at the entry point and throughout the distribution system (*41*).

Finally, an EPA web application, Generalized Read-Across (GenRA), was used to assess potential Cl–N–NO_2^- toxicity outcomes (see the supplementary materials) from in vivo studies (*42*, *43*). The results indicated potential positive in vivo toxicity effects in 84 categories: 29 chronic toxicity, 13 prenatal development toxicity, 11 multigenerational reproductive toxicity, 9 subacute repeat dose toxicity, and 22 subchronic toxicity. Coupled with Cl–N–NO_2^- presence in all chloraminated drinking waters tested at concentrations up to 120 μg/liter (table S3), occurrence and toxicity studies are warranted to assess its contribution to the potential public health risk suggested by epidemiological studies (*44*).

Conclusions

We have demonstrated here that Cl–N–NO_2^- is an inorganic chloramine decomposition product. It does not yet have a Chemical Abstracts Service (CAS) registry number (see the supplementary materials), forms under relevant drinking water chloramination conditions, and is present at microgram per liter levels. The proposed formation pathways (Fig. 3A) were consistent with the product synthesis using NO_2^+ as the nitrating agent, and this implicates the reactive nitrogen species pathway in chloramination (*14*). Because Cl–N–NO_2^- has a 2:2:1 nitrogen: oxygen: chlorine atom ratio, our prior work conclusions (*17*) can be extended to infer that Cl–N–NO_2^- inclusion in inorganic chloramine decomposition mass balances may close the oxygen mass balance and explain up to 98% of the nitrogen mass balance. Treatment strategies to curb Cl–N–NO_2^- and other reactive nitrogen species–mediated disinfection by-products [e.g., *N*-nitrosodimethylamine (*14*)] may include enhancing NH_2Cl stability and quenching HNO and ONOOH and/or its decomposition products (e.g., NO_2^+; Fig. 3A) during NH_2Cl decomposition. Because activated carbon was previously shown to destroy the UP by chemical reaction (*23*), point-of-entry and point-of-use home and building treatment systems containing activated carbon may chemically reduce Cl–N–NO_2^-, like its precursor, NH_2Cl (*45*). A GenRA simulation indicated that Cl–N–NO_2^- is a potential human health concern and is therefore an immediate candidate for quantitation in source waters, finished drinking waters, and wastewater effluents; assessment of its carcinogenicity and reproductive and developmental toxicities is also needed [e.g., (*44*, *46*, *47*)]. In addition to inorganic chloramine systems, occurrence studies should include other chlorine-based disinfectant schemes (e.g., free chlorine and chlorine dioxide) in which ammonia-nitrogen, nitrogen-containing NOM, or nitrogen-containing micropollutants are present [e.g., (*48*, *49*)].

REFERENCES AND NOTES

1. Centers for Disease Control and Prevention, "A century of US water chlorination and treatment: One of the ten greatest public health achievements of the 20th century" (2012); https://archive.cdc.gov/www_cdc_gov/healthywater/drinking/history.html.
2. S. W. Krasner *et al*., *J. Am. Water Works Assoc.* **81**, 41–53 (1989).
3. S. D. Richardson, M. J. Plewa, E. D. Wagner, R. Schoeny, D. M. Demarini, *Mutat. Res.* **636**, 178–242 (2007).
4. C. M. Villanueva *et al*., *Epidemiology* **15**, 357–367 (2004).
5. M. B. Rahman *et al*., *BMC Cancer* **14**, 445 (2014).
6. J. Grellier *et al*., *Epidemiology* **21**, 300–313 (2010).
7. K. Waller, S. H. Swan, G. DeLorenze, B. Hopkins, *Epidemiology* **9**, 134–140 (1998).
8. US Environmental Protection Agency, "National primary drinking water regulations: Stage 2 disinfectants and disinfection byproducts rule 71 FR 387 (2006); https://www.federalregister.gov/documents/2006/01/04/06-3/national-primary-drinking-water-regulations-stage-2-disinfectants-and-disinfection-byproducts-rule.
9. AWWA Disinfection Committee, *J. Am. Water Works Assoc.* **113**, 20–28 (2021).
10. C. J. Seidel, M. J. McGuire, R. S. Summers, S. Via, *J. Am. Water Works Assoc.* **97**, 87–97 (2005).
11. U.S. Environmental Protection Agency, "Summary of the public meeting of the Microbial and Disinfection Byproducts Rule Revisions Working Group, 20 September 2022; https://www.epa.gov/system/files/documents/2022-12/MDBP-Rule-Revisions-Working-Group-Meeting-Presentation-September-20-2022.pdf.
12. J. M. Allen *et al*., *Environ. Sci. Technol.* **56**, 392–402 (2022).
13. P. J. Vikesland, K. Ozekin, R. L. Valentine, *Water Res.* **35**, 1766–1776 (2001).
14. H. T. Pham, D. G. Wahman, J. L. Fairey, *Environ. Sci. Technol.* **55**, 1740–1749 (2021).
15. C. T. Jafvert, PhD Dissertation, University of Iowa, Iowa City, IA (1985).
16. C. T. Jafvert, R. L. Valentine, *Environ. Sci. Technol.* **26**, 577–586 (1992).
17. H. T. Pham, D. G. Wahman, J. L. Fairey, *Environ. Sci. Technol.* **58**, 2048–2057 (2024).
18. S. F. Leao, PhD Dissertation, University of California, Berkeley, Berkeley, CA (1981).
19. V. C. Hand, D. W. Margerum, *Inorg. Chem.* **22**, 1449–1456 (1983).
20. S. W. Leung, R. L. Valentine, *Water Res.* **28**, 1475–1483 (1994).
21. S. W. Leung, R. L. Valentine, *Water Res.* **28**, 1485–1495 (1994).
22. U.S. Environmental Protection Agency, "Comprehensive disinfectants and disinfection byproducts rules (stage 1 and stage 2): Quick reference guide" (EPA, 816-F-10-080, 2010); https://nepis.epa.gov/Exe/ZyPDF.cgi?Dockey=P100C8XW.txt.
23. R. L. Valentine, G. G. Wilber, in *Water Chlorination: Chemistry, Enviromental Impact and Health Effects*, R. L. Jolley, Ed. (International Water and Sanitation Centre, 1990), pp. 819–832.
24. S. S. Lau *et al*., *Environ. Sci. Technol.* **58**, 8654–8664 (2024).
25. R. L. Valentine, K. I. Brandt, C. T. Jafvert, *Water Res.* **20**, 1067–1074 (1986).
26. S. E. Hrudey, J. W. A. Charrois, *Disinfection By-Products and Human Health* (IWA Publishing and Australian Water Association, 2012).
27. M. Kirsch, H. G. Korth, A. Wensing, R. Sustmann, H. de Groot, *Arch. Biochem. Biophys.* **418**, 133–150 (2003).
28. D. L. McCurry, T. F. Speth, J. G. Pressman, *J. Environ. Eng.* **138**, 402–410 (2012).
29. US Environmental Protection Agency, "Definition and procedure for the determination of the method detection limit, revision 2" (EPA, 821-R-16-006, 2016); https://www.epa.gov/sites/default/files/2016-12/documents/mdl-procedure_rev2_12-13-2016.pdf.
30. S. E. Duirk, B. Gombert, J. P. Croué, R. L. Valentine, *Water Res.* **39**, 3418–3431 (2005).
31. P. J. Vikesland, K. Ozekin, R. L. Valentine, *Environ. Sci. Technol.* **32**, 1409–1416 (1998).
32. B. Martin Mousset, J. P. Croue, E. Lefebvre, B. Legube, *Water Res.* **31**, 541–553 (1997).
33. M. Loos, C. Gerber, F. Corona, J. Hollender, H. Singer, *Anal. Chem.* **87**, 5738–5744 (2015).
34. E. L. Schymanski *et al*., *Environ. Sci. Technol.* **48**, 2097–2098 (2014).
35. C. T. Jafvert, R. L. Valentine, *Water Res.* **21**, 967–973 (1987).
36. V. Shafirovich, S. V. Lymar, *Proc. Natl. Acad. Sci. U.S.A.* **99**, 7340–7345 (2002).
37. A. A. Lobanova, S. G. Il'yasov, G. V. Sakovich, *Russ. Chem. Rev.* **79**, 819–833 (2010).
38. M. Witanowski, L. Stefaniak, S. Szymanski, H. Januszewski, *J. Magn. Reson.* **28**, 217–226 (1977).
39. V. A. Shlyapochnikov *et al*., *J. Mol. Struct.* **559**, 147–166 (2001).
40. K. O. Christe *et al*., *Inorg. Chem.* **35**, 5068–5071 (1996).
41. American Water Works Association, "Nitrification prevention and control in drinking water (AWWA, manual M56 ed. 2, 2013); https://webstore.ansi.org/preview-pages/AWWA/preview_30056_M56_ed2.pdf.
42. I. Shah, J. Liu, R. S. Judson, R. S. Thomas, G. Patlewicz, *Regul. Toxicol. Pharmacol.* **79**, 12–24 (2016).
43. G. Patlewicz, I. Shah, *Comput. Toxicol.* **25**, 1–15 (2023).
44. R. J. Bull, D. A. Reckhow, V. Rotello, O. M. Bull, J. Kim, "Use of toxicological and chemical models to prioritize DBP research" (AWWA and EPA, project 2867, 2006); https://www.waterrf.org/research/projects/use-toxicological-and-chemical-models-prioritize-dbp-research.
45. J. L. Fairey, G. E. Speitel Jr., L. E. Katz, *Environ. Sci. Technol.* **40**, 4268–4273 (2006).
46. S. W. Krasner *et al*., *Environ. Sci. Technol.* **40**, 7175–7185 (2006).
47. B. I. Escher *et al*., *Environ. Sci. Technol.* **48**, 1940–1956 (2014).
48. J. F. Borsuah, T. L. Messer, D. D. Snow, S. D. Comfort, S. Bartelt-Hunt, *Sustainability (Basel)* **16**, 1181 (2024).
49. K. L. Klarich Wong *et al*., *Environ. Sci. Technol. Lett.* **6**, 98–105 (2019).

ACKNOWLEDGMENTS

We thank R. Murray, J. Pressman, T. Sanan, T. Speth, and J. Van Buren (EPA, Cincinnati, OH), D. Helbling (Cornell University), J. Podgorski [Swiss Federal Institute of Aquatic Science and Technology (Eawag), Duebendorf, Switzerland], E. Kolodziej (University of Washington), three anonymous reviewers for helpful comments on previous drafts of this manuscript; P. Longree (Eawag) for assistance with the IC–ESI–UHRMS method development and instrument operation; J. Hollender and H. Singer (Eawag) for helpful discussions regarding these methods; and A. Pifer (Garver, LLC) for organizing chloraminated drinking water sample collection. Research was not performed or funded by EPA and was not subject to EPA's quality system requirements. Views expressed are those of the authors and do not necessarily represent views or policies of EPA. **Funding:** This work was supported by the National Science Foundation (The NSF grant was awarded to J.L.F. only.); ETH-Zurich; and Eawag (sabbatical stipends to J.L.F.). **Author contributions:** Conceptualization: J.L.F., K.M., D.G.W.; Funding acquisition: J.L.F.; Investigation: J.L.F., J.R.L., H.T.P., T.D.D., S.D.H., K.M.; Methodology: J.L.F., J.R.L., K.M., D.G.W.; Project administration: J.L.F.; Supervision: J.L.F., K.M.; Visualization: J.L.F., J.R.L., K.M.; Writing – original draft: J.L.F., J.R.L., D.G.W.; Writing – review & editing: J.L.F., J.R.L., H.T.P., T.D.D., S.D.H., K.M., D.G.W. **Competing interests:** The authors declare no competing interests. **Data and materials availability:** All data are available in the main manuscript or the supplementary materials.

SUPPLEMENTARY MATERIALS

science.org/doi/10.1126/science.adk6749
Materials and Methods
Supplementary Text
Figs. S1 to S20
Tables S1 to S3
References (*50*–*64*)
MDAR Reproducibility Checklist

Submitted 30 October 2023; accepted 7 October 2024
10.1126/science.adk6749